

## Lattice-resolved frictional pattern probed by tailored carbon nanotubes

This article has been downloaded from IOPscience. Please scroll down to see the full text article.

2010 *Nanotechnology* 21 055702

(<http://iopscience.iop.org/0957-4484/21/5/055702>)

View the [table of contents for this issue](#), or go to the [journal homepage](#) for more

Download details:

IP Address: 140.109.103.227

The article was downloaded on 25/05/2011 at 04:28

Please note that [terms and conditions apply](#).

# Lattice-resolved frictional pattern probed by tailored carbon nanotubes

**Wei-Chiao Lai<sup>1,2,3</sup>, Shu-Cheng Chin<sup>1,3</sup>, Yuan-Chih Chang<sup>1</sup>, Li-Ying Chen<sup>1</sup> and Chia-Seng Chang<sup>1,2</sup>**

<sup>1</sup> Institute of Physics, Academia Sinica, Nankang, Taipei 115-29, Taiwan

<sup>2</sup> Department of Physics, National Taiwan University, Taipei 106-17, Taiwan

E-mail: [jasonc@phys.sinica.edu.tw](mailto:jasonc@phys.sinica.edu.tw) (C-S Chang)

Received 3 September 2009, in final form 29 November 2009

Published 21 December 2009

Online at [stacks.iop.org/Nano/21/055702](http://stacks.iop.org/Nano/21/055702)

## Abstract

In this study, we demonstrate a high-resolution friction profiling technique using synchronous atomic/lateral force microscopy (AFM/LFM). The atomic resolution is achieved by our special carbon nanotube (CNT) probes made via *in situ* tailoring and manipulation inside an ultra-high vacuum transmission electron microscope (UHV TEM). The frictional pattern mapped on graphite displays a periodic distribution similar to the atomic (0001)-oriented graphite lattice structure. Furthermore, the electrothermal process in the UHV TEM renders a graphite-capped CNT tip, which delivers the nanotribology study within two graphite layers by the LFM measurement on graphite. The synchronous AFM and LFM images can discern a spatial shift between the atomic points and local friction maxima. We further interpret this shift as caused by the lattice distortion, which in turn induces irreversible energy dissipation. We believe this is the origin of atomic friction on the sub-nanonewton scale.

 This article features online multimedia enhancements

(Some figures in this article are in colour only in the electronic version)

## 1. Introduction

While modern device fabrications demonstrate a predictive trend of continuous shrinking in the size of every component unit, problems concerning friction and wear start to pose a severe challenge at the nanometer scale. On this scale, traditional lubricants usually fail because of its serious viscosity and adhesiveness within a molecular thickness, which consequently cause damage to the miniature designed structures. Therefore, nanotribology, over the past five years, has become a prevalent issue for finding the solutions of nanoscale lubrication. In 2006, two significant achievements were highlighted for providing two promising approaches to reducing friction at the nanometer scale by control of the external parameters [1, 2]. One was achieved by Park *et al* in that the friction sensed by the tip of a scanning probe microscope (SPM) would vary with the tip bias and the sample doping level. They detected a palpable disparity in friction force when the tip scanned over the striped p-

doped regions on an originally n-doped silicon substrate [3]. The other was Socoliuc *et al*'s work which demonstrated a friction reduction proportional to the resonant amplitude of the tapping cantilever [4]. In their experiment, they applied a sinusoidal actuation to drive a tapping cantilever into resonance against a sliding contact. However, the required complicated design of either Socoliuc *et al*'s ultra-high vacuum (UHV) atomic force microscope (AFM) or Park *et al*'s combination AFM-scanning tunneling microscope (STM) has limited the nanotribology development in recent years [1]. So far, the friction at the atomic scale is still largely a mystery, and characterization of the nanoscale force interaction usually demands elaborate instruments. To popularize the study of intriguing nanotribology phenomena thus calls for a simpler and friendlier kind of scanning force microscopy (SFM). This kind of SFM must have high lateral force sensitivity, an imaging resolution close to the atomic level and operable under ambient conditions. Judging from these essential factors, improving the long-standing technique of lateral force microscopy (LFM) [5] seems to be a reasonable choice to suit our purpose.

<sup>3</sup> The two authors, W-C Lai and S-C Chin, contributed equally to this paper.

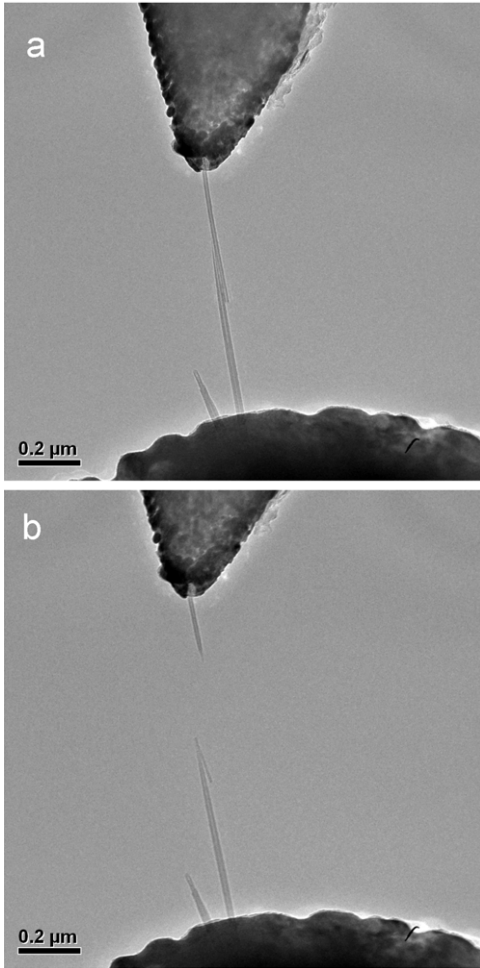


**Figure 1.** The TEM images demonstrate how we make a CNT probe suitable for the LFM measurement. (a) The remnant CNT on the gold STM tip can serve as a nanoknife to cut the CNT probe. (b) By carefully adjusting the bias and the resultant conducting current, the CNT probe can be tailored to a favorable dimension.

## 2. Carbon-nanotube-probed lateral force measurement

Although the conventional LFM is able to render frictional patterns close to atomic resolution, the measured periodic lateral force signals actually represent the averaged responses to the surface atomic periodicity. It is intuitive that a blunt tip, of which the apex diameter usually becomes much larger than 20 nm soon after the engagement of the contact-mode (CM) scan, cannot resolve the tip–sample force interaction within a  $10 \times 10 \text{ nm}^2$  area or less. Therefore, the well-known high-aspect-ratio carbon nanotube (CNT) probe should be a convenient candidate to solve the bluntness problem. Our recent technique has outlined a routine process to fabricate high-quality CNT probes with the telescope shape, which have reduced the typical artifacts found in the tapping-mode AFM measurement using a conventional longer and softer CNT probe [6]. When applied to the LFM measurement, the much stronger tip–sample interaction due to the contact will further disadvantage the use of a flexible CNT. We thus need to refine the CNT probe fabrication to a stricter dimension.

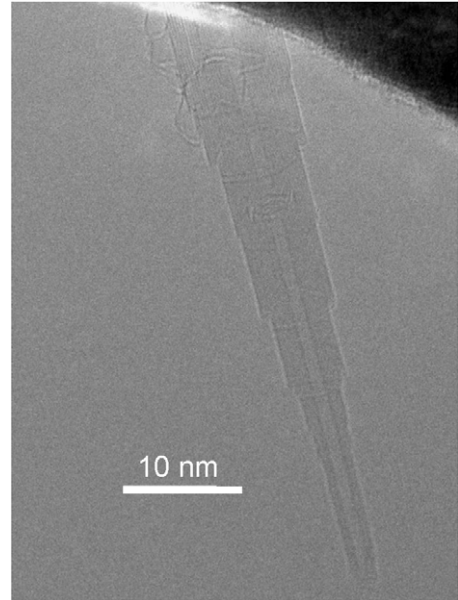


**Figure 2.** The TEM image displays a CNT probe specialized for the LFM experiment, which is done with the *in situ* tailoring process described in section 2.

In figure 1(a), two remnant CNTs are attached onto the commercial Au/Cr-coated or Pt/Ti-coated cantilever tip (upper), MikroMasch NSC 36, and the gold STM tip (lower), respectively. Initially, the two remnant CNTs belonged to one long CNT and were attached onto both tips. We then applied a voltage bias across them to generate a current flow through the CNT. When the current reached  $\sim 10 \mu\text{A}$ , the heat accumulated at roughly the central position burned the CNT off. The complete procedures of CNT probe fabrication were conducted in our UHV transmission electron microscope (TEM) (JEOL JEM-2000V) and described in [6].

Although we cut the long CNT in half, the CNT probe in figure 1(a) is obviously too long for the LFM measurement, which is normally performed under a tip–sample pressure up to  $\sim \text{GPa}$ . On this pressure order, CNT is relatively soft and flexible. We therefore let the remnant CNT touch the CNT probe and apply a bias onto the gold STM tip [7] (lower part in figure 1(a)). Then the resultant current burns off the CNT probe as figure 1(b) displays, where the cutoff segment can be seen on the lower CNT. Furthermore, we can judiciously adjust the current to tailor the tube apex into a user-defined dimension. For instance, a multi-walled CNT with a single-walled CNT’s sharpness can be achievable. The rigid multi-walled base gives strong support against the problematic lateral deformation in the later LFM experiments. While several methods have demonstrated how to cut and sharpen the CNTs using the Nanofactory machines [8], however, the high vacuum ( $\sim 10^{-7} \text{ mbar}$ ) inside the TEM chamber could still induce contamination of the CNT probe. The contamination is generally attributed to the heat generation during the current flow. In contrast, the UHV condition ( $< 5 \times 10^{-10} \text{ mbar}$ ) of our STM@TEM system eliminates this contamination problem. We thus produce a CNT probe with a well-defined telescope shape shown in figure 2, where a satisfactory apex of  $< 5 \text{ nm}$  can be seen. Also the rigid tip base with a  $\sim 50 \text{ nm}$  length,

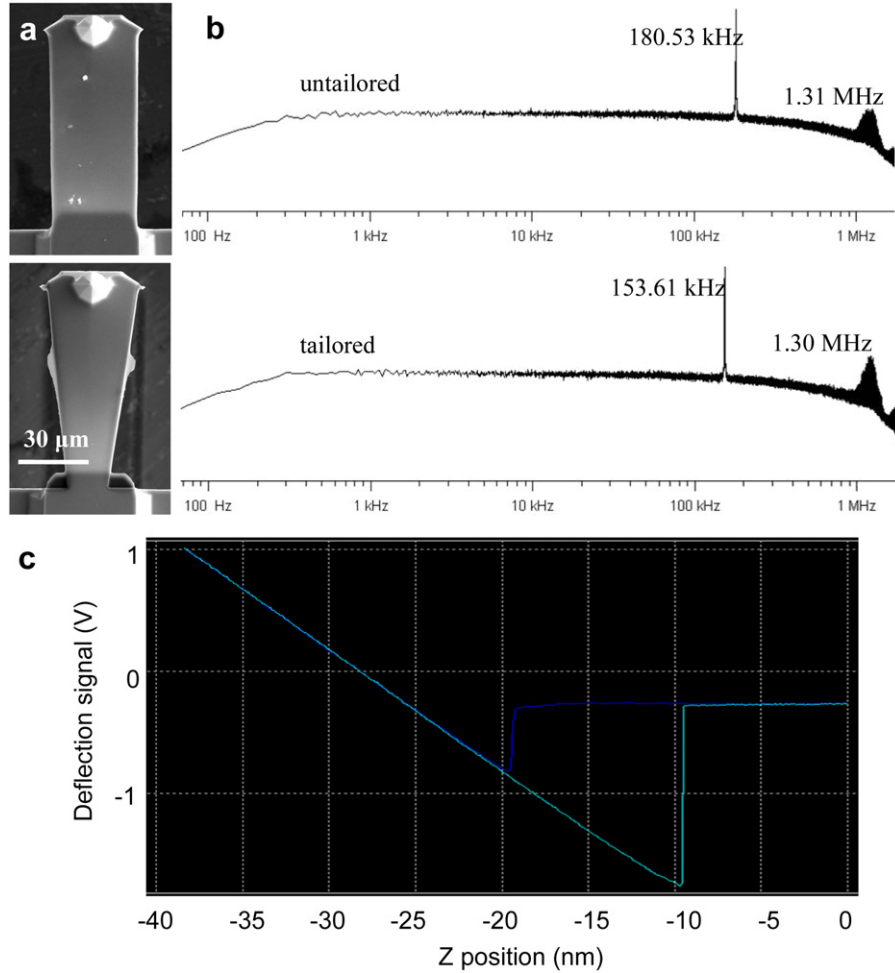


**Figure 3.** (a) The SEM images show the original rectangular silicon cantilever beam with Au/Cr coating (upper portion) was tailored by a commercial FIB instrument (lower portion). The tailored narrower neck is expected to enhance the torsional sensitivity during the lateral force measurement. (b) The resonant frequency spectra of untailored and tailored cantilevers tuned from the thermal measurements display individually the tapping and torsional frequency peaks. (c) The force curve demonstrates the position change in 10 nm gives the deflection voltage change in 1 V.

much shorter than the conventional ones (usually  $>100$  nm), can prevent the general CNT deformation during the lateral force measurement.

The entire LFM experiment was operated in a temperature-controlled room at  $\sim 21$  °C and with relative humidity  $<30\%$ . The total experimental time always took less than 1.5 h. Combined with the hydrophobicity of graphite itself, the possible surface water adhesion effect can thus be eliminated. In our case of the atomic friction measurement, we usually employ a normal force around 2–40 nN to produce a sensible lateral force. To sustain a tip–sample pressure up to  $\sim$ GPa, we hence choose the typical tapping-mode cantilevers with much higher spring constants than contact-mode ones. The pressure is supposed to induce sufficiently tight tribological sliding for the lateral force measurement and stresses again the necessity of our short CNT probe. Moreover, as the scanning electron microscopy (SEM) images show in figure 3(a), we tailored the original cantilever beam (upper portion) into a narrower neck (lower portion) with a commercial dual-beam focused-ion beam (FIB) instrument (FEI NOVA-600). This modified shape of a cantilever will have a higher torsional sensitivity.

The torsional spring constant is derived by the resonant frequency relation:  $2\pi f = (k/m)^{1/2}$ , which means  $k \propto f^2$ . The thermal measurements of the untailored and tailored cantilevers in figure 3(b) display two peaks individually in the spectra. For the tailored cantilever, the first harmonic frequency is at 153.6 kHz while the second one is at 1.3 MHz. It is known that the first and second harmonic frequencies of a rectangular beam with a free and fixed end correspond to the resonant frequencies of tapping and torsion [9]. Also the tapping spring constant from the thermal measurement is  $2.7 \text{ N m}^{-1}$ . The torsional spring constant is thus estimated as  $197 \text{ N m}^{-1}$ . Furthermore, the force curve in figure 3(c) demonstrates the slope that the position change of 10 nm gives the deflection voltage change of 1 V. In the later LFM experiments, we assume the lateral deflection is of the same linear relation as the vertical deflection. Referring to the estimated torsional spring constant, we can obtain a lateral deflection change in 1 mV corresponding to a lateral force  $\sim 2$  nN.

Figures 4(a)–(d) displays two typical CNT-probed AFM/LFM images with two different scan rates, i.e. 0.8 Hz

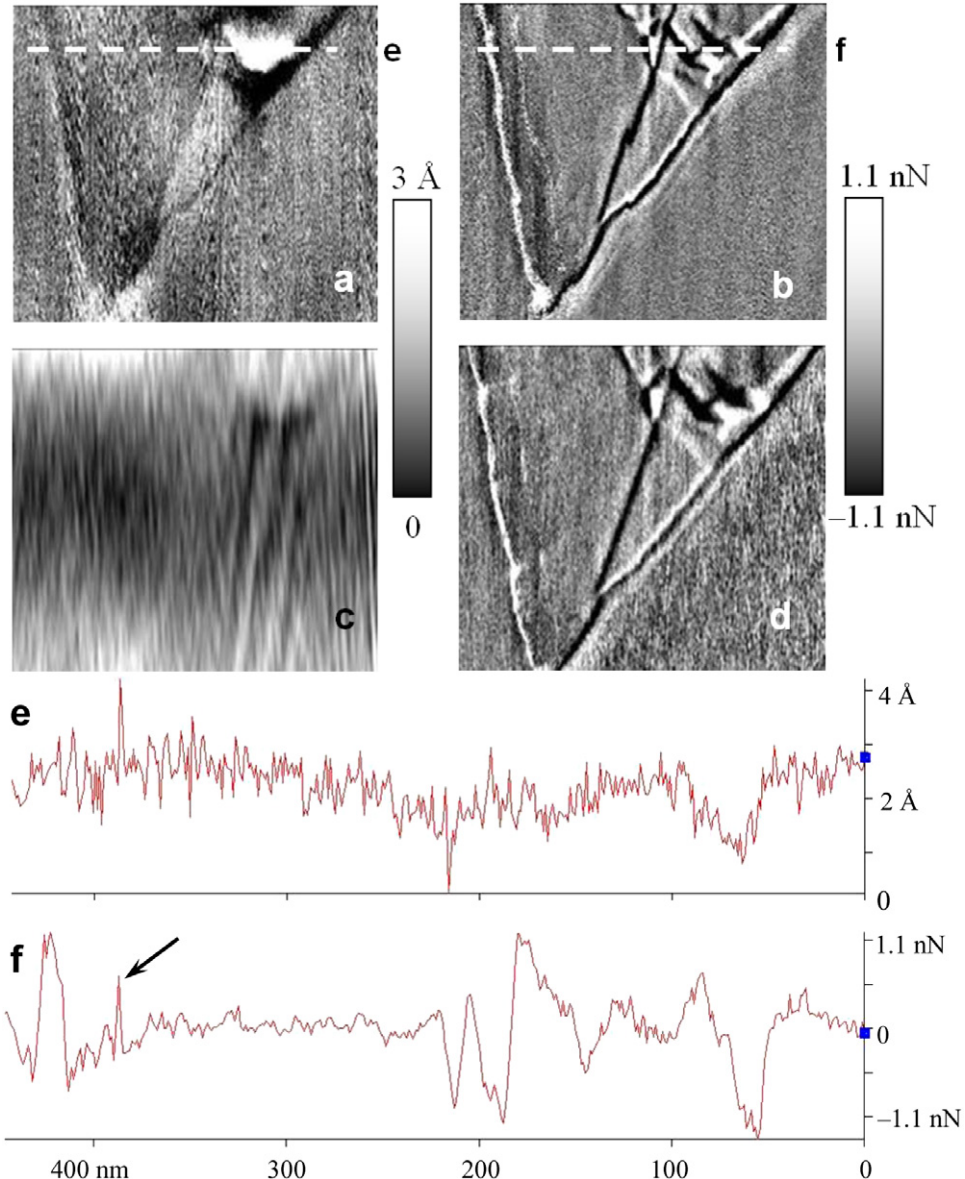


**Figure 4.** ( $500 \times 450 \text{ nm}^2$ ) Two typical CNT-probed AFM/LFM image sets with the scan rates of (a) and (b) 0.8 Hz, and (c) and (d) 10 Hz, respectively. We can recognize the disappearance of all the features at high speed. However, the lateral force measurement using the telescopic CNT probe attached to the FIB-tailored cantilever is apparently able to resolve tiny surface structures, like tiny fissures, with quite a sharp contrast in the LFM images (b) and (d). (e) and (f) The line scan profiles taken as the white dashed lines indicated in (a) and (b). The black arrow in (f) points out a feature with a size  $<5 \text{ nm}$ , which manifests the capability of our telescope-shaped CNT probe in figure 2.

for figures 4(a) and (b) and 10 Hz for figures 4(c) and (d). The AFM image in figure 4(a) displays an arbitrary tiny surface fracture coming from the sample preparation of cleaving the highly oriented pyrolytic graphite (HOPG). The small vibration of several ångströms in figure 4(a) may arise from the instability of the tailored cantilever under a slightly larger normal force around 3 nN. However, the scale bar for figures 4(a) and (c) still reveals the CNT probe's ability to profile the minute fissures, especially the extremely sharp lateral contrast in the LFM image (figure 4(b)). Even if we increase the scan rate up to 10 Hz, which makes the AFM topography (figure 4(c)) almost disappear, the corresponding LFM image (figure 4(d)) can still appear with a clear contrast. This benefits from the tailored cantilever with high torsional

sensitivity and the ultra-sharp CNT probe described in figures 2 and 3. Figures 4(e) and (f) display the line scan profiles taken at the white dashed lines indicated in figures 4(a) and (b). The line scan profile of the LFM image clearly demonstrates a superior contrast in comparison with that of the AFM image. More importantly, the black arrow in figure 4(f) evidently points out a feature with a size  $<5 \text{ nm}$ , which manifests the resolving ability of our telescope-shaped CNT probe in figure 2.

We further locate the CNT probe to some flat areas and zoom in to obtain the AFM/LFM images. Figure 5(a) shows a typical AFM image afflicted with vibrations of a few ångströms, whereas the LFM image in figure 5(b) clearly demonstrates the frictional pattern close to the atomic images

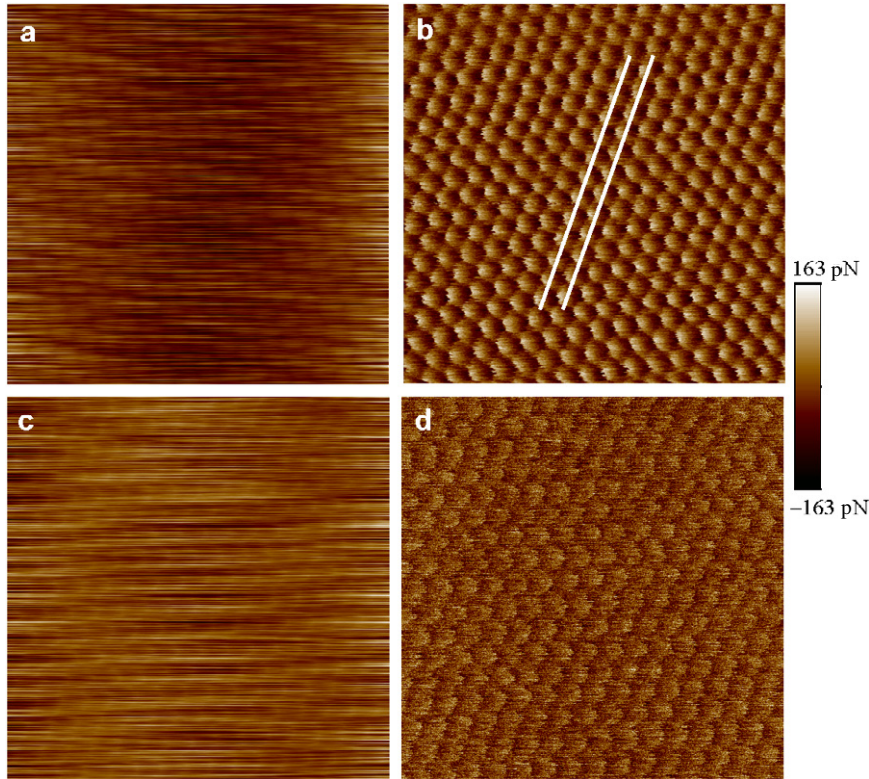


**Figure 5.** ( $4 \times 4 \text{ nm}^2$ ) The simultaneously scanned (a) AFM and (b) LFM images demonstrate the atomic resolution obtained by our *in situ* trimmed CNT probe at a 5 nN setpoint. The carbon–carbon distance of 2.5 Å is consistent with the previous STM and AFM experimental results. (c) and (d) The AFM/LFM image set taken with the naked FIB-tailored cantilever tip without CNT attachment in the lower panel of figure 3(a). Using a CNT probe, (b) clearly shows the superior contrast in comparison with (d).

of a graphite surface in the previous AFM or STM papers. The scan rate of figure 5 is set at 15 Hz against the thermal drift. Both the carbon–carbon distances of 2.5 Å in figures 5(a) and (b) are consistent with the previous explanations [10]. The white lines in figure 5(b) sketch the lattice spacing on a graphite surface, which will be discussed in the relevant text of figure 6. Figures 5(c) and (d) are the AFM/LFM image set obtained with the naked FIB-tailored cantilever tip, without CNT attachment, in the lower panel of figure 3(a). Comparing the images in figures 5(a)–(d), although both AFM images appear noisy, a CNT-probed LFM image in figure 5(b) clearly shows a better atomic contrast than figure 5(d) at the same force scale. That means the sharp CNT tip is able to enhance not only the spatial resolution but also the force sensitivity. From the aforementioned facts, it indicates that our CNT-probed LFM has the potential to map out high-resolution lateral roughness and atomic friction. Also it seems promising in understanding many mysterious nanoscale friction phenomena with an atomistic view.

### 3. Friction at the atomic scale

Figure 6 is the LFM images obtained with the tailored cantilever without CNT attachment. We first apply an ultra-large normal force around 50–100 nN to pick up a graphite flake. As shown in figure 6(a), the strips suddenly come along, when scanned from top to bottom, implying that a flake was

picked up. We then move the flake-attached tip to another flat area and start scanning with a setpoint of 30 nN. In figure 6(b), we can distinguish a strip spacing of 2.0 Å, which can be illustrated by the white lines in figure 5(b). The carbon–carbon distance is usually 2.5 Å in the conventional atomic graphite image. Therefore, the distance of the two parallel white lines is 2.1 Å, which accords with the 2.0 Å spacing in figure 6(b) and thus verifies that the strips are the lattice spacing on the (0001) graphite plane. The appearance of the lattice spacing in figure 6 agrees with the friction mapping by Dienwiebel *et al* [11], who discovered the origin of superlubrication lying in the incommensurability between rotated graphite layers. They mentioned in their paper that the tungsten tip they used would pick up a graphite flake, and then this flake would scan the graphite surface to obtain the frictional information between two sliding graphite sheets (or even two graphene sheets), but they failed to observe any clear image of subtle graphite flakes on their tungsten tip via any TEM imaging. They carried out a theoretical estimation and indicated that the graphite flake should have a dimension of 7–12 lattice spacings. Such a small graphite or even a graphene flake, attached onto a poly-metal surface, is in general impossible to be seen by a conventional TEM.

A CNT with a helical graphite structure itself, instead of a small graphite flake, should provide direct evidence about the contact between two graphite layers. We thus redid the same process in section 2 to produce a probe in figure 7. Here, we

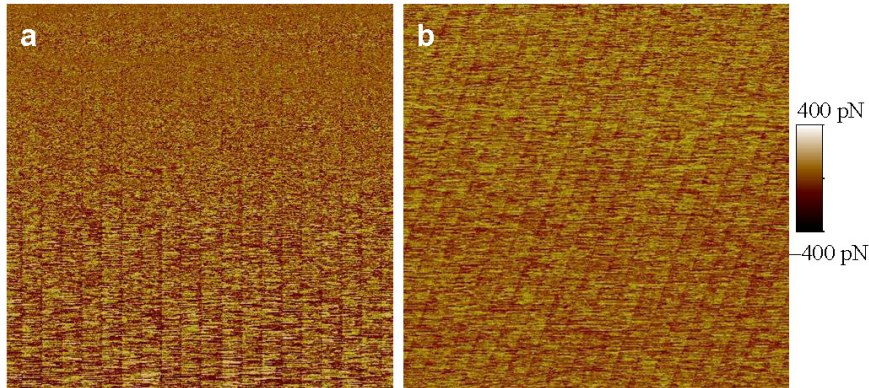


**Figure 6.** ( $4 \times 4 \text{ nm}^2$ ) (a) A LFM image taken with the naked tailored cantilever without CNT attachment displays the evident occurrence of lattice spacing after picking up a graphite flake. (b) The LFM image appears with a lattice spacing of  $2.0 \text{ \AA}$ , which is illustrated in figure 5(b).

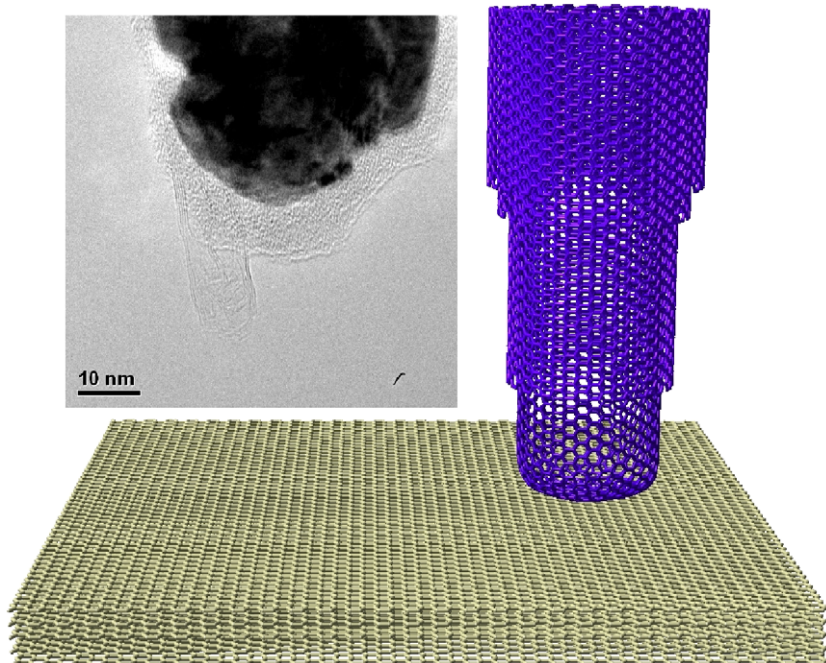


**Figure 7.** The high-resolution TEM image displays a short CNT length of  $10 \text{ nm}$  suitable for the atomic friction characterization. Next to the TEM image is a scheme which illustrates the expected scan mechanism between carbon nanotube and graphite. The closed-capped tube end is calculated under the lowest-energy solution to have the same structure as the graphite surface, which delivers the real graphite-graphite scan and in turn is able to clarify the nanotribology between two graphite (or even graphene) layers.

have to emphasize that the  $10 \text{ nm}$  length of the CNT probe is very important for the atomic friction measurement. Since it involves a tiny lateral force variation, we must engage a larger normal force, about  $30 \text{ nN}$ , to ensure a tight sliding and at the same time no CNT deformation [12]. In the traditional tribology studies, the unknown tip-sample asperity has always been a critical issue. The exact contact area within the tip-sample tribology needs to be identified to clarify the interaction within. Here, we evidently produced an atomically flat closed cap to achieve a single asperity, with a well-defined periodic surface, which allows the complete contact on another atomically flat surface. This closed cap was elaborated by letting the gold STM tip (figure 1) fully touch a user-selected CNT end [6] to slowly burn its length, roughly at a rate

of  $10 \text{ nm}$  per  $10 \text{ min}$ , the process of which is recorded in video 1 (available at [stacks.iop.org/Nano/21/055702/mmedia](http://stacks.iop.org/Nano/21/055702/mmedia)). By the deliberate control of the conducting current, it allows the heated carbon atoms to have enough kinetic energy to form the most stable structure at the cap region. This most stable structure is simulated via the software, Nanorex NanoEngineer-1, to render a hexagonal (0001)-oriented graphite structure under the lowest-energy approximation. The scheme in figure 7 explicitly illustrates how we delivered the expected graphite-graphite scan and it was drawn by the same simulation software. In comparison with the Nanofactory holders in conventional TEMs, the typical vacuum  $\sim 10^{-7} \text{ mbar}$  would additionally induce impurities within the closed cap, consequently polluting the hexagonal

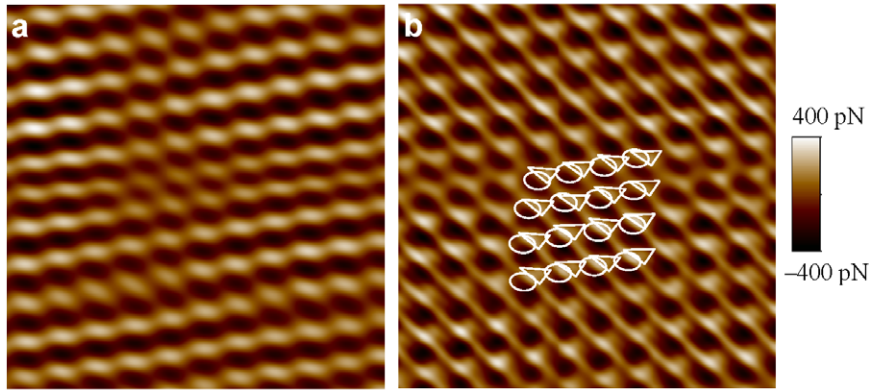


**Figure 8.** ( $2.5 \times 2.5 \text{ nm}^2$ ) (a) A CNT AFM image displays the atomic structure of graphite, where a slight thermal drift due to the low-speed scan can be observed. (b) The corresponding CNT LFM image of (a) appears with a similar periodic structure to (a), where a spatial shift between the atomic points and the friction maxima is depicted.

graphite crystallization. This will undoubtedly deteriorate the graphite-graphite mapping. The UHV technique seems to be the unique solution for this contamination issue. Although Bhushan and his co-workers have implemented the CNT-probed tapping-mode AFM to acquire the frictional information from the subtraction between the trace and retrace amplitude images of suspended CNTs [13], applications of CNT probes are still restricted in the domain of tapping-mode scanning force microscopy [14].

The lateral stiffness of the CNTs used in this paper should be estimated to support the absence of CNT deformation. The bending force constant of our CNT with 10 nm in diameter is given by  $k_{\text{CNT}} = 3YI/L^3$ , where  $Y = 0.5 \text{ TPa}$  is the Young's modulus,  $I = \pi(a^4 - b^4)/4$  is the inertia moment ( $a$  and  $b$  are outer and inner radii, respectively), and  $L$  is the exposed tube length [15]. Using this formula, the bending constants of the 50 nm and 10 nm long CNT are around  $56 \text{ N m}^{-1}$  and  $7000 \text{ N m}^{-1}$ , respectively, which are consistent with the previous measurement of the CNT bending constant [12]. In figure 5(b), the clear atomic image verifies that the bending effect of the CNT can be neglected. Most importantly, the  $7000 \text{ N m}^{-1}$  bending constant is much higher than the torsional constant of  $197 \text{ N m}^{-1}$ . Thus, the probe in figure 7 need not be worried about its flexibility and softness in the following measurements.

We further utilized the graphite-capped CNT probe in figure 7 to obtain the AFM/LFM images in figures 8(a) and (b). Here, the CNT probe has improved the reliability of the method developed by Dienwiebel *et al* [11] because the CNT cap is of a graphite structure itself. Consequently, we can be sure of the real graphite-graphite contact in every scan. In contrast, the geometry of a randomly picked graphite flake cannot be user-controlled, and it would be detrimental to the lattice-resolved frictional mapping once the corrugated flake was picked. Moreover, we do not have to worry the worn tungsten tip of 80 nm blunt as in the previous friction experiments [16]. Our method employing a commercially available LFM is much simpler than Dienwiebel *et al*'s homemade isotropic tip holder with a dual-laser deflection configuration.

Figures 8(a) and (b) are the CNT-probed AFM and LFM images that have been Fourier-filtered since the raw data of the

two images appear quite noisy. The noise could be attributed to the destruction of the rectangular cantilever beam. The beam has been tailored to a narrow neck for more sensitive torsion. At the same time, the deterioration in structural stability made this beam pose torsional vibration when an enormous normal force is employed. In this case,  $\sim 30 \text{ nN}$  is a very large force for the typical force measurement. That is also the reason why we choose the conventional tapping-mode cantilevers instead of contact-mode (CM) ones to engage a CM friction measurement, because the conventional CM cantilevers usually give no significant message but noise at such a large setpoint. The  $30 \text{ nN}$  induced vibration in the CM topography measurement leads to a fluctuation in the lateral deflection signals, comparable to the atomic friction signals on the order of sub-nanoneutron (shown in the scale bar of figure 8(b)). In addition to the lattice spacing shown in figure 6(b), the CNT-probed LFM image (figure 8(b)) reveals a similar periodic structure to the atomic AFM image in figure 8(a). In spite of a slight thermal drift in a few ångströms (the scan rate is 1 Hz for an image resolution of 512 pixels  $\times$  512 pixels), a spatial shift between the atomic points and the local lateral force maxima can be observed. As illustrated in figure 8(b), the ellipses in figure 8(b) represent the atomic points in figure 8(a) and the triangles represent the lateral force maxima. The spatial shift here is consistent with the previous experimental results disclosed by Ruan and Bhushan [17], who have explained that the shift may originate from the tip atom pushed by the lateral force.

Ruan and Bhushan further concluded that the atomic friction is a response to the energy dissipation within the interlayer electronic interaction [17]. Their derivation, under the hypothesis that the scanning tip is of a single-atom asperity, demonstrates the force field between the tip and surface is a conservative field. This conservative force in turn yields the energy dissipation proportional to a sinusoidal function with the same spatial period as the lattice constant of a surface structure. The energy dissipation is so reversible and renders an average zero dissipation across a unit cell, i.e. a respondent zero friction across a unit cell. Nevertheless, our graphite-capped CNT probe can be treated as a single asperity, but not as a single-atom asperity. Even so, we can still treat every atom

on the graphite cap as an individual single-atom asperity. The reason is the perfect lattice match between the two graphite layers. What if the single atom is one of the atoms on the graphite cap on the other side? The circumstance becomes that many periodically arranged atoms are sliding across a surface with the same periodicity. In other words, every atom on the cap suffers the same environment, just like a single atom. Consequently, the graphite-graphite scan here can be interpreted by Ruan and Bhushan's model.

Otherwise, in Dienwiebel *et al*'s experiment, they disclosed the superlubricity orientation in relation to the incommensurable and commensurable sliding between two graphite layers. Based on the perfect lattice match between two identical graphite sheets, the incommensurability between these two layers allows every atom to skid through the honeycomb lattice spacings on each other, consequently resulting in an ultra-low friction value that should ideally approach zero [18]. In our experiment, however, we cannot ascertain the incommensurability/commensurability, because our anisotropic rectangular cantilever beam would bring in the geometry effect when we change the scan angle with the piezotube scanner. Nonetheless, the stick-slip behavior was indeed observed as the perfect commensurable lattice accordance occurred. In general, we can regard our experiment as largely an incommensurable graphite-graphite scan.

Both aforementioned models suggest that the superlubrication approaching tens of piconewtons should occur in our experiment, but the force scale bar in figure 8(b) covers 800 pN, much higher than the superlubrication. We attribute this sub-nanonewton friction in figure 8(b) to three possible reasons. The first is the lattice distortion caused by the tip/surface atoms pushed/pulled by the lateral force or by the large tip–surface pressure, which simultaneously occur on both the CNT cap and the scanned graphite area. Such a distortion contributes to the local phonon effect, i.e. an additional amount of irreversible energy dissipation in heat into the entire crystal, which yields an average nonzero dissipation across any unit cell. In fact, this is nothing to do with the unit cell but with the number of atoms involved in the distortion. Simply speaking, more atoms involved in the lattice distortion lead to the higher friction. The second is that the amount of atoms on the CNT cap (10 nm in diameter) is roughly ten times Dienwiebel *et al*'s experiment done with a subtle graphite flake (7–12 lattice spacings in 1–2 nm or so). The recent theoretical modeling has shown a strong dependence of the amount of atoms involved in the atomic scale friction [19]. The third is the LFM working principle itself. The lateral force measurement works on a torsional cantilever tip, of which the necessary torque could cause another bending distortion of both graphite lattices and in turn to a crystal reorientation coupling to the lateral motion. In 2008 Filippov *et al* disclosed both theoretical and experimental results showing the reorientation-induced stabilization could lead the system to a high-friction state that eliminates the superlubrication [20].

All the AFM/LFM measurements in this paper were carried out by a commercially available multi-functional SFM system, Veeco Instruments diInnava, with the equipment of the Veeco NanoDrive controller. The thermal measurements and

figure 4 in this paper were done with another AFM system, Asylum Research MFP-3D, for its broader spectrum band width up to 5 MHz.

## 4. Conclusions

In summary, we have developed a convenient technique of the CNT-probed LFM to profile the atomic scale friction. In figures 4 and 5, the sharp contrast of the LFM images in comparison with the AFM images shows the feasibility of mapping out high-resolution lateral roughness within 5 nm and reaching atomic resolution. In addition, our graphite-capped CNT probe has guaranteed the complete contact area with the single asperity to study the nanotribological mechanism between two graphite layers. The periodic friction distribution at a sub-nanonewton scale displays the spatial shift between the graphite atomic positions in the AFM image and the local friction maxima in the LFM image, coming from the lateral force push/pull.

Finally, we have explained that the measured atomic friction originates from the irreversible tip–surface energy dissipation in relation to the lattice distortion. Moreover, the atom number involved and the torque-induced elimination of superlubrication have been discussed. The electrothermal process of the CNT probe in our UHV TEM fabricates a well-defined flat surface structure, which helps characterize many nanoscale tribology phenomena. We believe the application of our novel CNT probe to LFM will open a broad avenue for future nanotribology studies.

## Acknowledgments

The authors would like to thank Chi-Wen Yang and Hsien-Shun Liao in IPAS for their helpful discussions, and Pai-Chia Kuo for his technical assistance with FIB at the Academia Sinica Core Facilities for Nanoscience and Nanotechnology. This work is financially sponsored by the Academia Sinica Research Program on Nanoscience and Nanotechnology—Friction at the atomic scale.

## References

- [1] Frenken J 2006 *Nat. Nanotechnol.* **1** 20–1
- [2] Carpick R W 2006 *Science* **313** 184–5
- [3] Park J Y, Ogletree D F, Thiel P A and Salmeron M 2006 *Science* **313** 186
- [4] Socoliu A, Gnecco E, Maier S, Pfeiffer O, Baratoff A, Bennewitz R and Meyer E 2006 *Science* **313** 207–10
- [5] Mate C M, McClelland G M, Erlandsson R and Chiang S 1987 *Phys. Rev. Lett.* **59** 1942–5
- [6] Chin S C, Chang Y C and Chang C S 2009 *Nanotechnology* **20** 285307
- [7] Chang Y C, Liaw Y H, Huang Y S, Hsu T, Chang C S and Tsong T T 2008 *Small* **4** 2195–8
- [8] Wei X L, Chen Q, Liu Y and Peng L M 2007 *Nanotechnology* **18** 185503
- [9] Jeon S, Braiman Y and Thundat T 2004 *Appl. Phys. Lett.* **84** 1795–7
- [10] Tománek D, Louie S G, Mamin H J, Abraham D W, Thomson R E, Ganz E and Clarke J 1987 *Phys. Rev. B* **35** 7790–3
- [11] Dienwiebel M, Verhoeven G S, Pradeep N, Frenken J W M, Heimberg J A and Zandbergen H W 2004 *Phys. Rev. Lett.* **92** 126101

- [12] Ishikawa M, Yoshimura M and Ueda K 2002 *Physica B* **323** 184–6
- [13] Bhushan B, Ling X, Junge A and Hierold C 2008 *Phys. Rev. B* **77** 165428
- [14] Chin S C, Chang Y C, Chang C S, Woon W Y, Lin L T and Tao H J 2008 *Appl. Phys. Lett.* **93** 253102  
Chin S C, Chang Y C, Hsu C C, Lin W H, Wu C I, Chang C S, Tsong T T, Woon W Y, Lin L T and Tao H J 2008  
*Nanotechnology* **19** 325703
- [15] Akita S, Nishijima H, Kishida T and Nakayama Y 2000 *Japan. J. Appl. Phys.* **39** 3724–7
- [16] Dienwiebel M, Pradeep N, Verhoeven G S, Zandbergen H W and Frenken J W M 2005 *Surf. Sci.* **576** 197–211
- [17] Ruan J A and Bhushan B 1994 *J. Appl. Phys.* **76** 5022–35
- [18] Hirano M and Shinjo K 1990 *Phys. Rev. B* **41** 11837–51
- [19] Mo Y, Turner K T and Szlufarska I 2009 *Nature* **457** 1116–9
- [20] Filippov A E, Dienwiebel M, Frenken J W M, Klafter J and Urbakh M 2008 *Phys. Rev. Lett.* **100** 046102